Sodium/hydrogen exchanger NHA2 is critical for insulin secretion in β-cells

Christine Deisl[a,b,c], Alexandre Simonin[a,b,c], Manuel Anderegg[a,b,c], Giuseppe Albano[a,b,c], Gergely Kovacs[a,b], Daniel Ackermann[b,c], Holger Moch[d], Wanda Dolci[b,e], Bernard Thorens[b,e], Matthias A. Hediger[a,b], and Daniel G. Fuster[a,b,c,1]

[a]Institute of Biochemistry and Molecular Medicine and [b]Swiss National Centre of Competence in Research TransCure, University of Bern, 3012 Bern, Switzerland; [c]Division of Nephrology and Hypertension, University Hospital of Bern, 3010 Bern, Switzerland; [d]Institute of Clinical Pathology, University of Zürich, 8006 Zurich, Switzerland; and [e]Institute of Physiology, University of Lausanne, 1015 Lausanne, Switzerland

Edited by Gerald I. Shulman, Howard Hughes Medical Institute, Yale University, New Haven, CT, and approved May 1, 2013 (received for review November 17, 2012)

NHA2 is a sodium/hydrogen exchanger with unknown physiological function. Here we show that NHA2 is present in rodent and human β-cells, as well as β-cell lines. In vivo, two different strains of NHA2-deficient mice displayed a pathological glucose tolerance with impaired insulin secretion but normal peripheral insulin sensitivity. In vitro, islets of NHA2-deficient and heterozygous mice, NHA2-depleted Min6 cells, or islets treated with an NHA2 inhibitor exhibited reduced sulfonylurea- and secretagogue-induced insulin secretion. The secretory deficit could be rescued by overexpression of a wild-type, but not a functionally dead, NHA2 transporter. NHA2 deficiency did not affect insulin synthesis or maturation and had no impact on basal or glucose-induced intracellular Ca^{2+} homeostasis in islets. Subcellular fractionation and imaging studies demonstrated that NHA2 resides in transferrin-positive endosomes and synaptic-like microvesicles but not in insulin-containing large dense core vesicles in β-cells. Loss of NHA2 inhibited clathrin-dependent, but not clathrin-independent, endocytosis in Min6 and primary β-cells, suggesting defective endo–exocytosis coupling as the underlying mechanism for the secretory deficit. Collectively, our in vitro and in vivo studies reveal the sodium/proton exchanger NHA2 as a critical player for insulin secretion in the β-cell. In addition, our study sheds light on the biological function of a member of this recently cloned family of transporters.

Sodium/hydrogen exchangers [NHEs; solute carrier 9 (*Slc9*) gene family] exchange monovalent cations such as Na^+, Li^+, or K^+ with protons across lipid bilayers and are present in prokaryotes and eukaryotes (1). In mammals, 12 NHE isoforms are known so far (2). Recent additions to the large mammalian NHE family include NHA1 and NHA2, which possess higher homology to prokaryotic NHEs than the previously known NHEs 1–9 (2). Although NHA1 (also known as NHEDC1 or SLC9B1) is testis-specific, NHA2 (also known as NHEDC2 or SLC9B2) is widely expressed, including in the pancreas (3, 4). The physiological function of NHAs remains unknown. Based on chromosomal localization of the *NHA2* gene, transport characteristics, and inhibitor sensitivity, NHA2 was proposed to be the long-sought sodium/lithium countertransporter (3). Sodium/lithium countertransporter activity is a highly heritable trait that was linked to the development of essential hypertension and diabetes in humans (5, 6). Given the reported expression of NHA2 in the pancreas and the epidemiological evidence linking NHA2 to the pathogenesis of diabetes mellitus in humans, we carried out in vitro and in vivo experiments to define the role of NHA2 in the endocrine pancreas.

Results

NHA2 Is Expressed in Mouse and Human β-Cells. Immunofluorescence staining of mouse pancreatic cryosections revealed the presence of NHA2 in β-cells of Langerhans islets as assessed by colocalization with the marker insulin, whereas the NHA2 signal in the exocrine pancreas was very weak (Fig. 1*A*). The NHA2 staining detected in Langerhans islets of wild-type (WT) mice was absent in NHA2-deficient mice (Fig. 1*B*). At the mRNA and protein level we detected NHA2 in extracts of total pancreas as well as in isolated islets of WT mice, but not in pancreatic extracts or islets from two different lines of NHA2-deficient mice (Fig. 1 *C*–*F*). NHA1 expression was very low in islets and was not different between NHA2 WT and knock-out (KO) islets (Fig. S1). In addition, NHA2 was present in the mouse and rat β-cell lines Min6 and INS-1E, respectively (Fig. 1*G*). Finally, immunohistochemistry of paraffin-embedded human pancreatic sections also revealed NHA2 expression in human islets (Fig. 1*H*).

Knockdown of NHA2 in Min6 Cells Reduces Secretagogue-Induced, but Not Direct Depolarization-Induced, Insulin Secretion. To test whether NHA2 plays a role in insulin secretion, we first used RNA interference to reduce endogenous NHA2 levels in Min6 cells. Knockdown of NHA2 was maximal 72 h after transfection and typically reached ∼70–80% (Fig. 2*A*). Whereas basal insulin secretion was unaffected by a reduction in NHA2 levels, glucose- and sulfonylurea-induced insulin secretion were significantly reduced (Fig. 2*B*). Knockdown of NHA2, however, did not affect direct depolarization-induced insulin secretion elicited by an increase of extracellular K^+. Insulin and proinsulin contents of Min6 cells with NHA2 knockdown were unchanged (Fig. 2 *C* and *D*). We next attempted to rescue the effect of NHA2 knockdown in Min6 cells by simultaneous overexpression of WT or functionally dead human NHA2 or the empty control vector (Fig. 2*E* and Fig. S2) (3). siRNAs used to target murine NHA2 had no sequence homology to human NHA2 mRNA. As shown in Fig. 2*E*, overexpression of WT, but not functionally dead, human NHA2 rescued the insulin secretion deficit induced by knockdown of endogenous NHA2 in Min6 cells. These results suggest that, at least in vitro, NHA2 indeed plays a role in insulin secretion by inhibiting secretagogue-induced, but not depolarization-induced, insulin secretion in Min6 cells.

Impaired Glucose Tolerance and Insulin Secretion in NHA2 KO and Heterozygous Mice. To examine the role of NHA2 in vivo, we studied two groups of transgenic, NHA2-deficient mice. Mice with a retroviral genetrap in intron 1 of the *NHA2* gene, herein named NHA2 genetrap mice ($NHA2^{gt}$), were generated and described previously by our group (7). For this study, we also generated targeted NHA2 KO mice (herein named NHA2 KO mice) by a conventional homologous recombination approach resulting in

Author contributions: C.D., M.A.H., and D.G.F. designed research; C.D., A.S., M.A., G.A., G.K., D.A., H.M., W.D., and D.G.F. performed research; G.K. and B.T. contributed new reagents/analytic tools; C.D., M.A., G.A., G.K., H.M., B.T., M.A.H., and D.G.F. analyzed data; and D.G.F. wrote the paper.

The authors declare no conflict of interest.

This article is a PNAS Direct Submission.

[1]To whom correspondence should be addressed. E-mail: Daniel.Fuster@ibmm.unibe.ch.

This article contains supporting information online at www.pnas.org/lookup/suppl/doi:10.1073/pnas.1220009110/-/DCSupplemental.

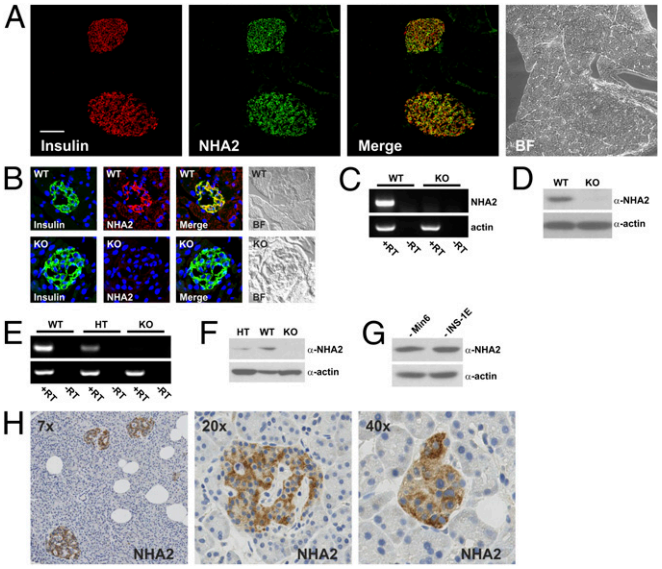

Fig. 1. NHA2 is present in murine and human β-cells. (*A*) Pancreatic cryosection stained for insulin (red) and NHA2 (green) with colocalization (yellow) in the merged image. Bright-field (BF) image is shown on the right. (Scale bar: 50 μm.) (*B*) Murine islets from WT and NHA2 genetrap (KO) mice stained for insulin (green) and NHA2 (red), with yellow indicating colocalization in the merged image. BF images are shown on the right. (*C*) RT-PCR for NHA2 and actin from pancreatic mRNA isolated from WT and NHA2 genetrap mice. (*D*) Immunoblot for NHA2 and actin of pancreatic protein extracts from WT and NHA2 genetrap mice. (*E*) RT-PCR for NHA2 and actin from pancreatic mRNA from WT, heterozygous, and NHA2 KO mice. (*F*) Immunoblot for NHA2 and actin of isolated islets (100 islets per lane) from WT, heterozygous, and NHA2 KO mice. (*G*) Immunoblot of mouse Min6 and rat INS-1E cell lysates for NHA2 and actin. (*H*) Immunohistochemical staining for NHA2 in human paraffin-embedded pancreatic tissue.

loss of exon 7 of the *NHA2* gene. Exon 7 codes for two aspartic acid residues that have been shown to be paramount for NHA2 function (3, 8) (Fig. S2). As shown in Fig. 1 *B*–*F*, NHA2 protein and mRNA were undetectable in the pancreas or in isolated islets of both lines of NHA2-deficient mice.

We first evaluated the impact of *NHA2* gene inactivation on disposal of a glucose load by i.p. glucose tolerance tests (IPGTT) in both lines of transgenic mice. As shown in Fig. 3*A*, compared with WT mice, both NHA2 KO and heterozygous mice exhibited higher glycemic excursion following an i.p. glucose load (2 g of glucose per kg of body weight). Similar findings were obtained with NHA2 genetrap mice (Fig. 3*D*) or with fully backcrossed NHA2 KO mice (Fig. S3). Corresponding serum insulin levels (including basal) were lower in NHA2 genetrap mice throughout the IPGTT and in NHA2 KO mice at 15 and 30 min after the glucose challenge compared with WT mice, consistent with an insulin secretion defect (Fig. 3 *B* and *E* and Fig. S3). In contrast, fasting serum glucagon levels were identical in WT and NHA2 genetrap mice (Fig. S4). Interestingly, heterozygous mice exhibited a phenotype that was similar to KO mice during the IPGTT (Fig. 3 *A* and *B*). To exclude the possibility that the observed glucose intolerance was the result of peripheral insulin resistance, we performed i.p. insulin tolerance tests (IPITT) in both groups of transgenic mice. As shown in Fig. 3 *C* and *F*, both groups of transgenic mice exhibited a peripheral insulin sensitivity that was not different from their respective WT littermates. There was even a trend to increased glucose sensitivity in NHA2 KO mice (Fig. 3*C*). There were no significant genotype differences in average weights of mice used for IPGTT and IPITT experiments, respectively (Table S1). Together, these data are compatible with the notion that loss of NHA2 results in impaired glucose tolerance due to a defect of insulin secretion in vivo.

Reduced Insulin Secretion of Islets from NHA2-Deficient Mice. A myriad of factors, however, can affect insulin secretion and glucose tolerance in vivo. To further delineate the role of NHA2 in insulin secretion, we performed insulin secretion assays using isolated islets. Insulin secretion was measured in static batch incubations for 2 h, and KCl-induced secretion was studied for 1 h. As shown in Fig. 4*A*, 20 mM glucose-induced insulin secretion was greatly reduced in heterozygous and NHA2 KO islets. Both in heterozygous and KO islets, basal insulin secretion was also significantly reduced compared with WT islets. Similar results were obtained for tolbutamide-induced insulin secretion with significantly less insulin secreted in KO and heterozygous islets compared with WT islets (Fig. 4*B*). We next also investigated the effect of direct (supraphysiological) depolarization-induced insulin secretion by addition of 50 mM KCl to the incubation buffer (with concomitant equimolar reduction of the NaCl concentration). As seen before in Min6 cells, depolarization-induced insulin secretion did not differ in the three groups of islets (Fig. 4*C*). Similar findings were obtained with islets isolated from NHA2 genetrap mice (Fig. S5) and from backcrossed NHA2 KO mice (Fig. S6). Dynamic islet perifusion experiments furthermore revealed that loss of NHA2 attenuated both first- and second-phase insulin secretion; the kinetics of insulin secretion of NHA2 KO islets, however, were indistinguishable from WT islets (Fig. 4*D*). Islet insulin and proinsulin contents in WT, heterozygous, and KO islets were identical (Fig. 4 *E*–*G*). Both pancreatic and islet insulin content were also not different between WT and NHA2 genetrap mice (Fig. S7), suggesting that insulin synthesis and maturation are normal in NHA2-deficient islets.

Phloretin is an inhibitor of NHA2 but also of Glut-2, which is essential for glucose-induced insulin secretion in β-cells (3, 9). At a concentration of 180 μM, phloretin was previously shown to inhibit insulin release stimulated by glucose and tolbutamide but not by KCl-induced depolarization (10). At this dose, which completely inhibits NHA2 transport activity in a functional NHA2 transport assay (Fig. S2), phloretin was reported to not affect the oxidation rate of glucose, the rate of glucose utilization, or the islet content of ATP. Furthermore, a cell-impermeable phloretin–dextran compound was still able to inhibit glucose-stimulated insulin secretion

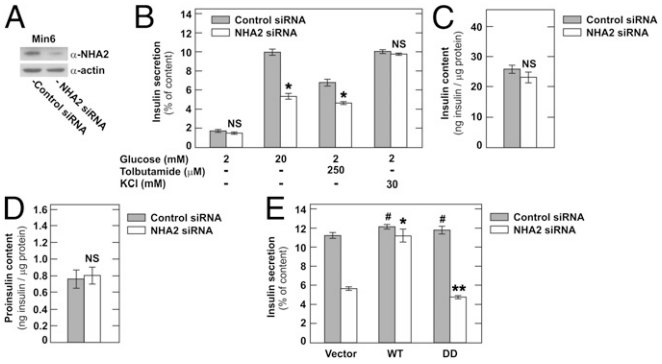

Fig. 2. Knockdown of NHA2 in Min6 cells inhibits secretagogue-induced insulin secretion. (*A*) Typical immunoblot of Min6 cells treated with control or NHA2-targeting siRNA. (*B*) Insulin secretion normalized to insulin content of Min6 cells transfected with control or NHA2-targeting siRNA. Data are means ± SEM (n = 8–12 per condition). *$P < 0.05$ vs. control; NS, not significant. (*C* and *D*) Insulin (*C*) and proinsulin (*D*) content of Min6 cells treated with control or NHA2-targeting siRNA. Data are means ± SEM (n = 10–12 per condition). NS, not significant. (*E*) Glucose-induced insulin secretion of Min6 cells cotransfected with control or NHA2-targeting siRNA and WT, functionally dead (DD) HA-tagged human NHA2, or empty vector. Data are means ± SEM (n = 8 per condition). *$P < 0.05$ vs. combined empty vector and NHA2 siRNA transfected; **NS vs. combined empty vector and NHA2 siRNA transfected; #NS vs. combined empty vector and control siRNA transfected.

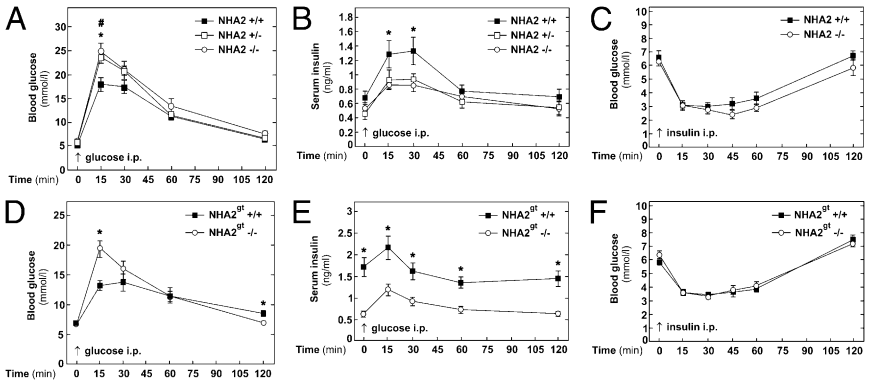

Fig. 3. Glucose and insulin tolerance test in NHA2 KO and genetrap mice. (*A*) Blood glucose levels measured in whole blood following i.p. glucose challenge (2 g per kg of body weight) in KO mice and heterozygous and WT littermates ($n^{+/+} = 12$; $n^{+/-} = 10$; $n^{-/-} = 10$). Data are means ± SEM. *$P < 0.05$, WT vs. KO; #$P < 0.05$, WT vs. heterozygous. (*B*) Insulin concentration measured in sera of KO mice and heterozygous and WT littermates following i.p. glucose challenge (2 g per kg of body weight) ($n^{+/+} = 9$; $n^{+/-} = 10$; $n^{-/-} = 10$). Data are means ± SEM. *$P < 0.05$, WT vs. KO. (*C*) Blood glucose levels measured in whole blood following i.p. insulin challenge (1 U per kg of body weight) in KO mice and WT littermates ($n^{+/+} = 12$; $n^{-/-} = 12$). Data are means ± SEM. (*D*) Blood glucose levels measured in whole blood following i.p. glucose challenge in genetrap NHA2 mice and WT littermates (NHA2$^{gt\ -/-}$ and NHA2$^{gt\ +/+}$, respectively; $n^{+/+} = 12$; $n^{-/-} = 12$). Data are means ± SEM. *$P < 0.05$, WT vs. NHA2-deficient. (*E*) Insulin concentration measured in sera of genetrap NHA2 mice and WT littermates following i.p. glucose challenge (2 g per kg of body weight) ($n^{+/+} = 12$; $n^{-/-} = 12$). Data are means ± SEM. *$P < 0.05$, WT vs. NHA2-deficient. (*F*) Blood glucose levels measured in whole blood following i.p. insulin challenge (1 U per kg of body weight) in genetrap NHA2 mice and WT littermates ($n^{+/+} = 9$; $n^{-/-} = 11$). Data are means ± SEM.

but was no longer active in inhibiting tolbutamide-mediated insulin secretion (10). We thus reasoned that, in addition to Glut-2, NHA2 may be a second, intracellular target of phloretin in β-cells. To test this hypothesis, we compared tolbutamide- and KCl-mediated insulin secretion in NHA2 WT and KO islets in the presence of 180 μM phloretin or its vehicle. As shown in Fig. 4*H*, whereas NHA2 KO islets were unaffected by phloretin treatment, phloretin inhibited tolbutamide-stimulated insulin secretion in NHA2 WT islets to the level of KO islets. Phloretin, however, had no effect on KCl-induced insulin secretion in WT or KO islets (Fig. 4*I*). These findings extend previous data on the phloretin effect in β-cells and indicate that NHA2 is indeed a second phloretin target. Together, these data indicate that loss or inhibition of NHA2 in islets inhibits insulin secretion.

NHA2 Localizes to Endosomes and Synaptic-Like Microvesicles in β-Cells. To study the intracellular localization of NHA2, we first performed subcellular fractionation experiments. Equilibrium density centrifugation of Min6 homogenates in linear sucrose gradients indicated that NHA2 was not present in the insulin-containing large dense core vesicle (LDCV) fraction (Fig. 5 *A* and *B*). LDCVs were detected by their insulin content and the presence of the LDCV marker carboxypeptidase E. Also, we found no NHA2 signal in the mitochondrial (marker: F-ATPase) or lysosomal fractions [marker: lysosomal-associated membrane protein 1 (Lamp-1)]. Instead, NHA2 localized with markers of endosomes [markers: Rab4, early endosome antigen 1 (EEA1), and transferrin receptor] and synaptic-like microvesicles (SLMVs; marker: synaptophysin). Similar results were obtained with the

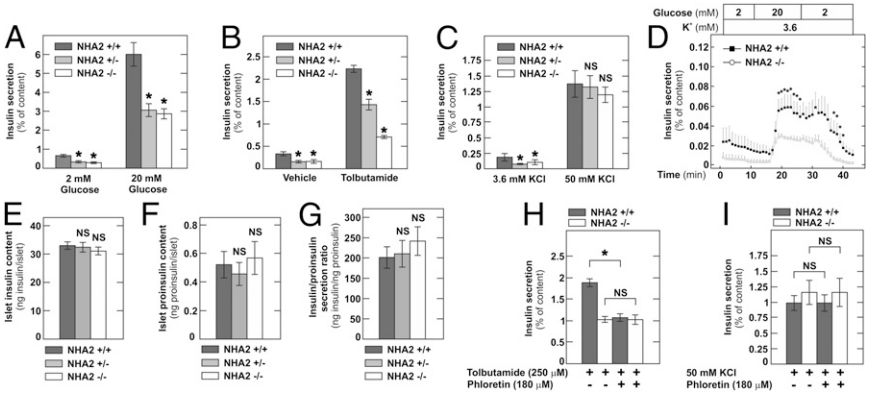

Fig. 4. Reduced secretagogue-induced insulin secretion in NHA2-deficient islets. (*A*) Basal and glucose-induced (20 mM) insulin release by isolated islets of NHA2 KO mice and heterozygous or WT littermates normalized to insulin content ($n = 18$ per genotype and condition). Data are means ± SEM. *$P < 0.05$ vs. WT. (*B*) Tolbutamide-induced (250 μM) insulin release by isolated islets of NHA2 KO mice and heterozygous or WT littermates normalized to insulin content ($n = 8$ per genotype and condition). Data are means ± SEM. *$P < 0.05$ vs. WT. (*C*) KCl-induced (50 mM) insulin release by isolated islets of NHA2 KO mice and heterozygous or WT littermates normalized to insulin content ($n = 8$ per genotype and condition). Data are means ± SEM. *$P < 0.05$ vs. WT; NS, not significant. (*D*) Insulin secretion of perifused islets of NHA2 WT ($n = 7$) and KO mice ($n = 7$) by low (2 mM) and high (20 mM) glucose. Data are means ± SEM. *$P < 0.05$ vs. KO. (*E*) Islet insulin content ($n = 68$ per genotype). (*F*) Islet proinsulin content ($n = 24$ per genotype). (*G*) Ratio of insulin vs. proinsulin secretion in 20 mM glucose ($n = 12$ per genotype). Data are means ± SEM. (*H*) Effect of 180 μM phloretin or vehicle (DMSO) on tolbutamide-induced (250 μM) insulin secretion in NHA2 KO mice and WT littermates normalized to insulin content ($n = 10$ per genotype). Data are means ± SEM. *$P < 0.05$; NS, not significant. (*I*) Effect of 180 μM phloretin or vehicle (DMSO) on KCl-induced (50 mM) insulin secretion in NHA2 KO mice and WT littermates normalized to insulin content ($n = 10$ per genotype). Data are means ± SEM. NS, not significant.

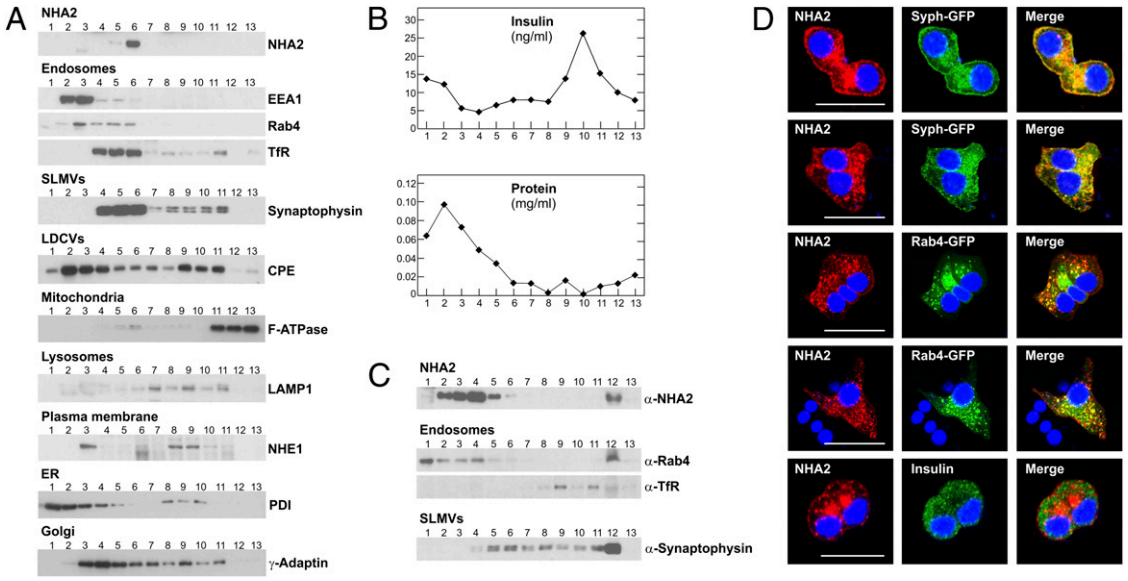

Fig. 5. NHA2 localizes to endosomes and SLMVs. (*A*) Subcellular fractionation of Min6 cells on a linear sucrose gradient. Thirteen fractions (from top to bottom) were collected after sucrose gradient centrifugation, and equal volumes of each fraction were analyzed by immunoblotting with antibodies directed against NHA2, EEA1, Rab4, transferrin receptor (TfR; endosomal markers), synaptophysin (SLMV marker), carboxypeptidase E (CPE; LDCV marker), F-ATPase α-subunit (mitochondrial marker), LAMP1 (lysosomal marker), NHE1 (plasma membrane marker), protein disulfide–isomerase (PDI; endoplasmic reticulum marker), and γ-adaptin (trans-Golgi network marker). (*B*) Protein and insulin concentration (as additional marker for LDCVs) of individual fractions. (*C*) Glycerol velocity gradient fractionation to separate endosomes and SLMVs. Fraction 1 corresponds to the top of the gradient. Equal volumes of each fraction were analyzed by immunoblotting with indicated antibodies. (*D*) Confocal images of Min6 cells transfected with HA-tagged NHA2 and GFP-tagged synaptophysin or GFP-tagged Rab4 or counterstained with anti-insulin antibody. Colocalization is indicated by yellow in merged images. (Scale bars: 20 μm.)

rat β-cell line INS-1E (Fig. S8). To better resolve endosomes and SLMVs, nonequilibrium glycerol velocity gradient experiments were performed. In these gradients, NHA2 was present in fractions enriched for endosomal markers but also in fractions that contained SLMVs and were devoid of endosomes, indicated by the presence of synaptophysin and absence of Rab 4 and transferrin in fractions 5 and 6 (Fig. 5*C*). To verify results obtained by subcellular fractionation experiments, we next conducted confocal imaging studies in Min6 cells. Unfortunately, our attempts to stain endogenous NHA2 in Min6 cells resulted in a poor signal-to-noise ratio. To circumvent this issue, we transfected HA-tagged NHA2 into Min6 cells (Fig. 5*D*). Clearly, NHA2 did not localize to insulin-containing vesicles, but there was substantial colocalization of NHA2 with the cotransfected, GFP-tagged endosomal marker Rab4 or the SLMV marker synaptophysin. Given the localization of NHA2 to SLMVs, we next assessed cellular content and secretion of γ-aminobutyric acid (GABA), the major constituent of SLMVs in β-cells (11). Identical experimental conditions as used for glucose-induced insulin secretion assays depicted in Fig. 4 were used. As shown in Fig. S9, GABA content and GABA secretion of KO islets were not different from WT islets. Thus, collectively, these data indicate that NHA2 localizes to endosomes and SLMVs in β-cells but is dispensable for GABA secretion.

NHA2 Is Critical for Clathrin-Dependent Endocytosis. Because of its endosomal localization, we reasoned that NHA2 may primarily affect endocytosis in β-cells, with an indirect impact on LDCV exocytosis. Previous reports demonstrated that endocytosis and exocytosis are tightly coupled in β-cells, with inhibition of endocytosis resulting in a decrease in insulin secretion (12, 13). We therefore next tested clathrin-dependent as well as clathrin-independent endocytotic pathways in Min6 cells with siRNA-mediated knockdown of NHA2. As shown in Fig. 6 *A* and *C*, clathrin-dependent endocytosis as assessed by the uptake of Alexa Fluor-568–labeled transferrin was significantly reduced in Min6 cells with NHA2 knockdown. In contrast, clathrin-independent (but dynamin-dependent) endocytosis of cholera toxin B as well as coat-independent fluid phase endocytosis (marker: lysine-fixable Texas Red–dextran 3000 MW) were not affected by knockdown of NHA2 in Min6 cells (Fig. 6 *B–D*). As in Min6 cells, uptake of transferrin was found to be reduced in primary β-cells isolated from NHA2 WT and KO mice (Fig. 6*E* and Fig. S10). As determined by confocal imaging, endocytosed transferrin colocalized both with synaptophysin and NHA2 in Min6 cells (Figs. S11 and S12). Overexpression of WT human NHA2, but not the empty vector, almost completely rescued the endocytosis deficit observed in NHA2-depleted Min6 cells (Fig. 6*F*). To test whether the NHE NHA2 participates in the regulation of endosomal pH, we performed fluorescence ratio imaging analysis of endosomes using transferrins labeled with two different fluorescent probes (FITC and Alexa Fluor 568) (14). As shown in Fig. 6 *G* and *H*, however, NHA2 depletion in Min6 cells or β-cells did not affect the steady-state pH of transferrin-positive endosomes. Together, these data indicate that endosomal NHA2 is critical for clathrin-dependent endocytosis in Min6 and primary β-cells, but not for regulation of endosomal pH.

Loss of NHA2 Does Not Change Cellular Ca^{2+} Homeostasis. Our functional observation that insulin secretion was unaltered by supraphysiological KCl concentration-mediated β-cell depolarization, but reduced with tolbutamide stimulation, suggested that the defect induced by loss of NHA2 was downstream of K_{ATP} channel closure but upstream of the final exocytotic event. K_{ATP} channel closure-induced depolarization of the β-cell leads to activation of voltage-sensitive L-type Ca^{2+} channels, with a subsequent rise of intracellular Ca^{2+}, which itself then drives vesicular exocytosis (15). We thus tested whether the glucose-elicited increase of intracellular Ca^{2+} was affected by loss of NHA2. As shown in Fig. S13 *A* and *B*, however, both basal and peak glucose-induced increases in intracellular Ca^{2+} were not different in NHA2 KO islets compared with WT islets. Disturbed

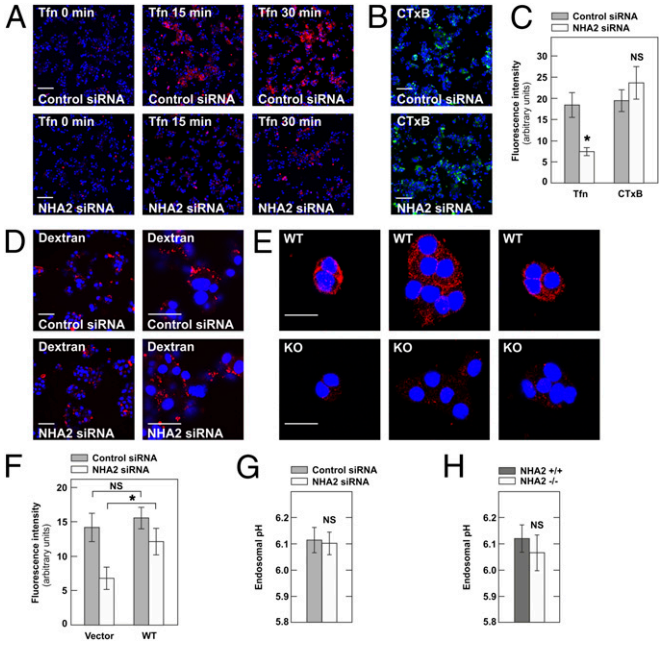

Fig. 6. NHA2 is required for clathrin-dependent endocytosis in Min6 and β-cells. (*A*) Transferrin–Alexa Fluor 568 (Tfn; red) uptake in Min6 cells treated with control (*Upper*) or NHA2-targeting siRNA (*Lower*) for indicated time. (Scale bars: 100 μm.) (*B*) Cholera toxin B–Alexa Fluor 488 (CTxB; green) uptake for 30 min in Min6 cells treated with control or NHA2-targeting siRNA. (Scale bars: 100 μm.) (*C*) Quantification of transferrin–Alexa Fluor 568 and cholera toxin B–Alexa Fluor 488 uptake for 30 min in Min6 cells treated with control or NHA2-targeting siRNA. Data are means ± SD of three experiments. $*P < 0.05$; NS, not significant. (*D*) Fluid-phase uptake assay performed in Min6 cells treated with control or NHA2-targeting siRNA by incubation for 30 min with lysine-fixable Texas Red–Dextran before fixation. Images are representative of three experiments. [Scale bars: 100 μm (*Left*) or 30 μm (*Right*).] (*E*) Transferrin–Alexa Fluor 568 (red) uptake for 30 min in primary β-cells isolated from NHA2 WT (WT) and KO (KO) mice. (Scale bars: 20 μm.) β-cells were identified by costaining with anti-insulin antibody (Fig. S10). Images are representative of three experiments. (*F*) Quantification of transferrin–Alexa Fluor 568 uptake for 30 min in Min6 cells treated with control or NHA2-targeting siRNA and transfected with control plasmid (vector) or WT NHA2 (WT). Data are means ± SD of three experiments. $*P < 0.05$; NS, not significant. (*G*) pH of transferrin-positive perinuclear endosomes in Min6 cells treated with control or NHA2-targeting siRNA ($n = 6$ per condition, pooled from two experiments). Data are means ± SEM. NS, not significant. (*H*) pH of transferrin-positive perinuclear endosomes in WT and NHA2 KO β-cells ($n = 21$ per condition, pooled from three experiments). Data are means ± SEM. NS, not significant.

intracellular Ca^{2+} handling therefore cannot explain the discrepancy observed between KCl- and secretagogue-induced insulin secretion in NHA2-deficient β-cells. The KCl stimulation protocol leads to massive activation of Ca^{2+} channels, with Ca^{2+} equilibration throughout the β-cell and subsequent release of any release-competent granules irrespective of their proximity to Ca^{2+} channels (16, 17). In islets, KCl-induced insulin secretion alone was far less than observed with sulfonylurea or glucose stimulation (Fig. 4) and may primarily induce the release of a special pool of predocked vesicles where NHA2 function is not required (16, 17). To test this hypothesis, we first incubated islets in high-glucose (20 mM) buffer for 15 min to deplete the ready-releasable granule pool and then performed high-KCl (50 mM) stimulation. As shown in Fig. S13*C*, KCl stimulation after high-glucose stimulation elicited a significantly lower secretory response in NHA2 KO islets compared with WT islets. Thus, depolarization-induced insulin secretion is not universally preserved in NHA2-deficient β-cells. Rather, this finding suggests that KCl stimulation alone preferentially induces a rapid and nonsustained release of predocked vesicles. Alternatively, in the absence of physiological secretagogues, high KCl may induce NHA2-independent endocytosis pathways that compensate for the loss of NHA2. Under physiological conditions, however, our data clearly demonstrate the requirement of NHA2 for insulin secretion, both in vitro and in vivo.

Discussion

Min6 cells with siRNA-mediated knockdown of NHA2, as well as islets isolated from NHA2-deficient mice, displayed reduced secretagogue-induced insulin secretion in static as well as dynamic insulin secretion experiments. Reduced secretagogue-induced insulin secretory capacity of NHA2-deficient β-cells evoked a pathological glucose tolerance in vivo. Interestingly, heterozygous mice were not normal but exhibited a clear phenotype in the glucose tolerance tests compared with WT mice, and islets isolated from heterozygous mice had reduced secretagogue-induced insulin secretion compared with WT islets. These data indicate that the level of NHA2 expression in β-cells is critical for insulin secretion and suggest a haploinsufficient mechanism for the observed insulin secretion deficit in heterozygous mice and islets.

Confocal imaging and subcellular fractionation studies demonstrated that NHA2 localizes to endosomes and SLMVs, which is in agreement with our previous observations in osteoclasts, in which NHA2 colocalized with markers of the endocytotic pathway (7). In support of the subcellular localization studies, functional experiments revealed that clathrin-dependent endocytosis was specifically inhibited when NHA2 was acutely (siRNA in Min6 cells) or chronically (primary β-cells of NHA2 KO mice) missing. However, we were unable to detect changes in the pH of transferrin-positive endosomes in NHA2 siRNA-treated Min6 cells or in β-cells of NHA2 KO mice. Although technical issues in the endosomal pH determination approach may theoretically have been the cause for this result, the method used is widely utilized and well established, and our pH measurements of transferrin-positive endosomes were in the range observed by others (18–22). Thus, the role of NHA2 in the endosome may not be regulation of pH, but control of endosomal cation concentration or pH sensing with subsequent recruitment of ancillary proteins that participate in vesiculation or trafficking events.

Exocytosis and endocytosis are tightly coupled in β-cells, and glucose was shown to stimulate simultaneously exocytosis of insulin granules and endocytosis in primary β-cells and INS-1E cells (23, 24). In contrast, inhibition of endocytosis by various approaches reduced insulin secretion (12, 25). Both LDCV and SLMV membrane proteins recycle back from the plasma membrane through endosomal intermediates with intermixing and temporal cohabitation (26, 27). However, whereas SLMVs can bud either directly from the plasma membrane or alternatively from endosomal intermediates, LDCV membrane proteins are recycled from the plasma membrane via endosomes through the trans-Golgi network for incorporation into new granules (28, 29). The additional SLMV biogenesis pathway avoiding endosomal intermediates may explain the fact that we could not detect differences in GABA secretion between WT and KO islets. However, we cannot exclude the possibility that we missed a real difference in GABA secretion between WT and KO islets due to spatial and temporal resolution limitations of the GABA secretion assay used (11).

Analysis of NHA2-neighboring genes on murine chromosome 3 revealed unaltered expression of NHA1 but increased expression of 3-hydroxybutyrate dehydrogenase (BDH2) (Fig. S1) in NHA2 KO islets. BDH2 is the enzyme responsible for the synthesis of the siderophore 2,5-dihydroxybenzoic acid, and loss of BDH2 in mammalian cells has been shown to lead to cytoplasmic iron accumulation and iron deficiency in mitochondria

(30). However, this view on the role of 2,5-dihydroxybenzoic acid as a siderophore in cellular iron homeostasis was challenged in a recent article (31). Human (and hominidae primate) BDH2 mRNA, but not rodent BDH2 mRNA, contains an iron-responsive element in the 3′ untranslated region, and cellular iron deficiency increases BDH2 mRNA in human but not rodent cells (32). Thus, BDH2 function in iron homeostasis is still under debate, and the regulation of BDH2 expression in species other than the hominidae family is currently unclear. Given the observed reduction in transferrin receptor endocytosis upon loss of NHA2, it is possible that there is a link between iron homeostasis and BDH2 expression in murine islets, and this possibility will need to be addressed in future studies. Theoretically, it is also possible that the NHA2 transgene enhances BDH2 transcription directly. However, the fact that siRNA-mediated knockdown of NHA2 in Min6 cells (no transgene effect) leads to similar findings as observed with NHA2-depleted islets makes a significant transgene-mediated and NHA2-independent contribution to the phenotype very unlikely.

Our in vitro and in vivo data reveal a critical role of the endosomal NHE NHA2 for clathrin-mediated endocytosis and insulin secretion in β-cells. The results of our study are compatible with a model whereby loss of NHA2 affects insulin secretion indirectly by interfering with clathrin-mediated endocytosis in β-cells, thereby disrupting endo–exocytosis coupling. Furthermore, our study sheds light on the biological function of a member of this recently cloned SLC9B family of transporters.

Methods

Additional experimental procedures are provided in *SI Methods*.

Isolation of Islets and in Vitro Insulin Release Assays. Pancreata were perfused in situ with collagenase solution, and islets were isolated exactly as described (33). After overnight incubation in RPMI medium with 11 mM glucose, islets were washed twice with Krebs–Ringer bicarbonate Hepes buffer (KRBH; pH 7.4) containing 2 mM glucose and then placed in 12-well plates (10 islets per well) containing 1 mL of KRBH with 2 mM glucose and preincubated for 2.5 h at 37 °C. Insulin secretion into KRBH was measured for 2 h for all secretagogues except for KCl, which was >1 h. After this time, supernatants were harvested, plates were put on ice, and total cellular insulin was extracted by the addition of acid ethanol [70% (vol/vol) ETOH, 1.5% (vol/vol) HCL conc. (=12.5%)]. Islet perifusion was performed as described (34). Batches of 30 islets were placed in parallel perifusion chambers at 37 °C and perifused at a flow rate of 1 mL/min with KRBH and indicated glucose and potassium concentrations. Fractions were collected every minute. At the end of the perifusion experiment, islets were collected and lysed by acidic ethanol. Secreted and cellular insulin (CrystalChem) and proinsulin (Mercodia ELISA) were determined by ELISA.

In Vivo Experiments. Blood glucose and/or insulin concentrations were measured in 8- to 12-wk-old male mice after a 3:00 to 9:00 AM 6-h fast (IPGTT) or at random-fed state at 2:00 PM (IPITT) as described (35, 36). Blood glucose was measured before and after i.p. injections of glucose (2 g/kg) or insulin (1 U/kg Actrapid HM; Novo Nordisk) with a Contour glucose monitor (Bayer Healthcare) by tail vein sampling at indicated time points in duplicates. Serum insulin (CrystalChem) and plasma glucagon (ALPCO Diagnostics) concentrations were determined by ELISAs.

ACKNOWLEDGMENTS. We thank Felix Frey and Claes Wollheim for helpful advice and fruitful discussions. D.G.F. was supported by Swiss National Science Foundation Grant 3100A0-117732, the Swiss National Centre of Competence in Research (TransCure), the Novartis Research Foundation, and a Prof. Dr. Max Cloëtta Foundation Medical Research Position Award.

1. Orlowski J, Grinstein S (2004) Diversity of the mammalian sodium/proton exchanger SLC9 gene family. *Pflugers Arch* 447(5):549–565.
2. Brett CL, Donowitz M, Rao R (2005) Evolutionary origins of eukaryotic sodium/proton exchangers. *Am J Physiol Cell Physiol* 288(2):C223–C239.
3. Xiang M, Feng M, Muend S, Rao R (2007) A human Na+/H+ antiporter sharing evolutionary origins with bacterial NhaA may be a candidate gene for essential hypertension. *Proc Natl Acad Sci USA* 104(47):18677–18681.
4. Fuster DG, et al. (2008) Characterization of the sodium/hydrogen exchanger NHA2. *J Am Soc Nephrol* 19(8):1547–1556.
5. Mangili R, et al. (1988) Increased sodium-lithium countertransport activity in red cells of patients with insulin-dependent diabetes and nephropathy. *N Engl J Med* 318(3): 146–150.
6. Canessa M, Adragna N, Solomon HS, Connolly TM, Tosteson DC (1980) Increased sodium-lithium countertransport in red cells of patients with essential hypertension. *N Engl J Med* 302(14):772–776.
7. Hofstetter W, Siegrist M, Simonin A, Bonny O, Fuster DG (2010) Sodium/hydrogen exchanger NHA2 in osteoclasts: Subcellular localization and role in vitro and in vivo. *Bone* 47(2):331–340.
8. Schushan M, et al. (2010) Model-guided mutagenesis drives functional studies of human NHA2, implicated in hypertension. *J Mol Biol* 396(5):1181–1196.
9. Uldry M, Thorens B (2004) The SLC2 family of facilitated hexose and polyol transporters. *Pflugers Arch* 447(5):480–489.
10. Ashcroft SJ, Nino S (1978) Effects of phloretin and dextran-linked phloretin on pancreatic islet metabolism and insulin release. *Biochim Biophys Acta* 538(2):334–342.
11. Braun M, et al. (2004) Regulated exocytosis of GABA-containing synaptic-like microvesicles in pancreatic beta-cells. *J Gen Physiol* 123(3):191–204.
12. Min L, et al. (2007) Dynamin is functionally coupled to insulin granule exocytosis. *J Biol Chem* 282(46):33530–33536.
13. Tomas A, Yermen B, Min L, Pessin JE, Halban PA (2006) Regulation of pancreatic beta-cell insulin secretion by actin cytoskeleton remodelling: Role of gelsolin and cooperation with the MAPK signalling pathway. *J Cell Sci* 119(Pt 10):2156–2167.
14. Ohgaki R, Fukura N, Matsushita M, Mitsui K, Kanazawa H (2008) Cell surface levels of organellar Na+/H+ exchanger isoform 6 are regulated by interaction with RACK1. *J Biol Chem* 283(7):4417–4429.
15. Barg S, et al. (2001) Fast exocytosis with few Ca(2+) channels in insulin-secreting mouse pancreatic B cells. *Biophys J* 81(6):3308–3323.
16. Collins SC, et al. (2010) Progression of diet-induced diabetes in C57BL6J mice involves functional dissociation of Ca2(+) channels from secretory vesicles. *Diabetes* 59(5): 1192–1201.
17. Hoppa MB, et al. (2009) Chronic palmitate exposure inhibits insulin secretion by dissociation of Ca(2+) channels from secretory granules. *Cell Metab* 10(6):455–465.
18. Xinhan L, et al. (2011) Na+/H+ exchanger isoform 6 (NHE6/SLC9A6) is involved in clathrin-dependent endocytosis of transferrin. *Am J Physiol Cell Physiol* 301(6): C1431–C1444.
19. Casey JR, Grinstein S, Orlowski J (2010) Sensors and regulators of intracellular pH. *Nat Rev Mol Cell Biol* 11(1):50–61.
20. Baravalle G, et al. (2005) Transferrin recycling and dextran transport to lysosomes is differentially affected by bafilomycin, nocodazole, and low temperature. *Cell Tissue Res* 320(1):99–113.
21. Barriere H, et al. (2009) Revisiting the role of cystic fibrosis transmembrane conductance regulator and counterion permeability in the pH regulation of endocytic organelles. *Mol Biol Cell* 20(13):3125–3141.
22. Gagescu R, et al. (2000) The recycling endosome of Madin-Darby canine kidney cells is a mildly acidic compartment rich in raft components. *Mol Biol Cell* 11(8):2775–2791.
23. Orci L, Malaisse-Lagae F, Ravazzola M, Amherdt M, Renold AE (1973) Exocytosis-endocytosis coupling in the pancreatic beta cell. *Science* 181(4099):561–562.
24. MacDonald PE, Eliasson L, Rorsman P (2005) Calcium increases endocytotic vesicle size and accelerates membrane fission in insulin-secreting INS-1 cells. *J Cell Sci* 118(Pt 24): 5911–5920.
25. Kimura T, et al. (2008) The GDP-dependent Rab27a effector coronin 3 controls endocytosis of secretory membrane in insulin-secreting cell lines. *J Cell Sci* 121(Pt 18): 3092–3098.
26. Partoens P, et al. (1998) Retrieved constituents of large dense-cored vesicles and synaptic vesicles intermix in stimulation-induced early endosomes of noradrenergic neurons. *J Cell Sci* 111(Pt 6):681–689.
27. Strasser JE, Arribas M, Blagoveshchenskaya AD, Cutler DF (1999) Secretagogue-triggered transfer of membrane proteins from neuroendocrine secretory granules to synaptic-like microvesicles. *Mol Biol Cell* 10(8):2619–2630.
28. Hannah MJ, Schmidt AA, Huttner WB (1999) Synaptic vesicle biogenesis. *Annu Rev Cell Dev Biol* 15(15):733–798.
29. Schmidt A, Hannah MJ, Huttner WB (1997) Synaptic-like microvesicles of neuroendocrine cells originate from a novel compartment that is continuous with the plasma membrane and devoid of transferrin receptor. *J Cell Biol* 137(2):445–458.
30. Devireddy LR, Hart DO, Goetz DH, Green MR (2010) A mammalian siderophore synthesized by an enzyme with a bacterial homolog involved in enterobactin production. *Cell* 141(6):1006–1017.
31. Correnti C, et al. (2012) Siderocalin/Lcn2/NGAL/24p3 does not drive apoptosis through gentisic acid mediated iron withdrawal in hematopoietic cell lines. *PLoS ONE* 7(8): e43696.
32. Liu Z, et al. (2012) Siderophore-mediated iron trafficking in humans is regulated by iron. *J Mol Med* 90(10):1209–1221.
33. Li DS, Yuan YH, Tu HJ, Liang QL, Dai LJ (2009) A protocol for islet isolation from mouse pancreas. *Nat Protoc* 4(11):1649–1652.
34. Preitner F, et al. (2004) Gluco-incretins control insulin secretion at multiple levels as revealed in mice lacking GLP-1 and GIP receptors. *J Clin Invest* 113(4):635–645.
35. Andrikopoulos S, Blair AR, Deluca N, Fam BC, Proietto J (2008) Evaluating the glucose tolerance test in mice. *Am J Physiol Endocrinol Metab* 295(6):E1323–E1332.
36. Brüning JC, et al. (1997) Development of a novel polygenic model of NIDDM in mice heterozygous for IR and IRS-1 null alleles. *Cell* 88(4):561–572.